

# Artificial Intelligence for Science, Industry, and Society

## AISIS - 2019

# Variational Autoencoders for Medical Imaging

Juan J. Cerrolaza, PhD  
accenturetechnology  
artificialintelligence IBERIA



Imperial College  
London

KING'S  
College  
LONDON

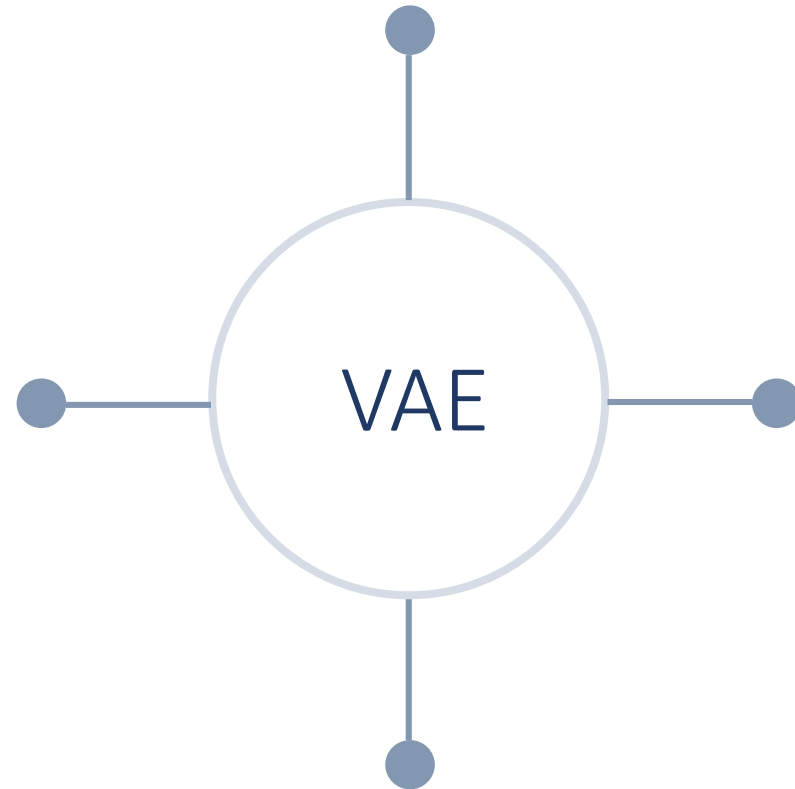


Children's National™  
Sheikh Zayed Institute  
for Pediatric Surgical Innovation  
Part of the Children's National Health System

accenture

# Variational Autoencoders - Background

Neural Network Perspective



Dimensionality Reduction  
Method

Generative Model

Probability Model Perspective

# Variational Autoencoders - Background

Dimensionality Reduction  
Method



Generative Model

# Variational Autoencoders - Background

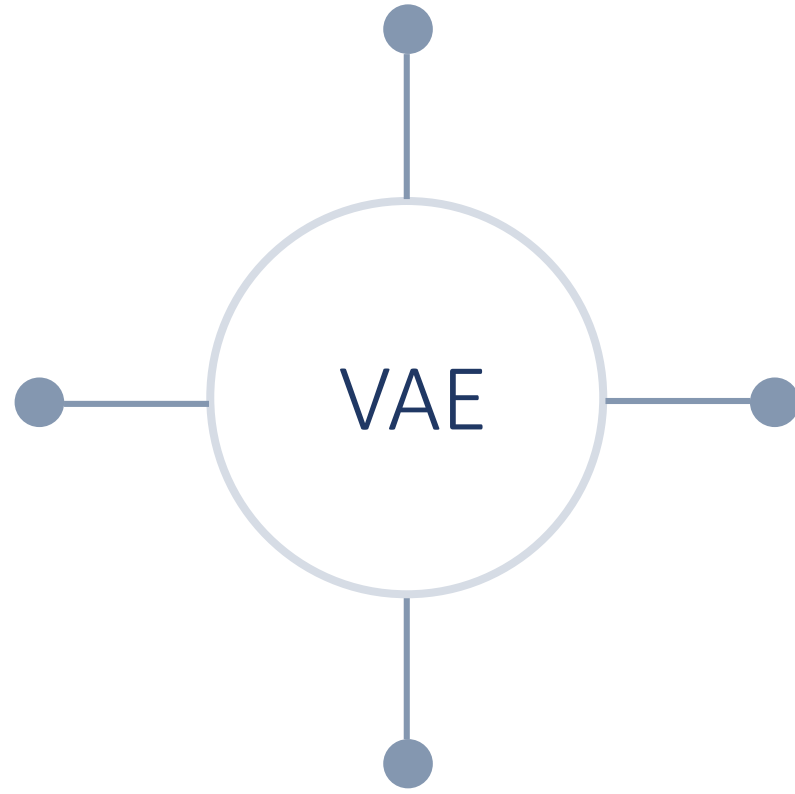
Neural Network Perspective



Probability Model Perspective

# Variational Autoencoders - Background

Neural Network Perspective



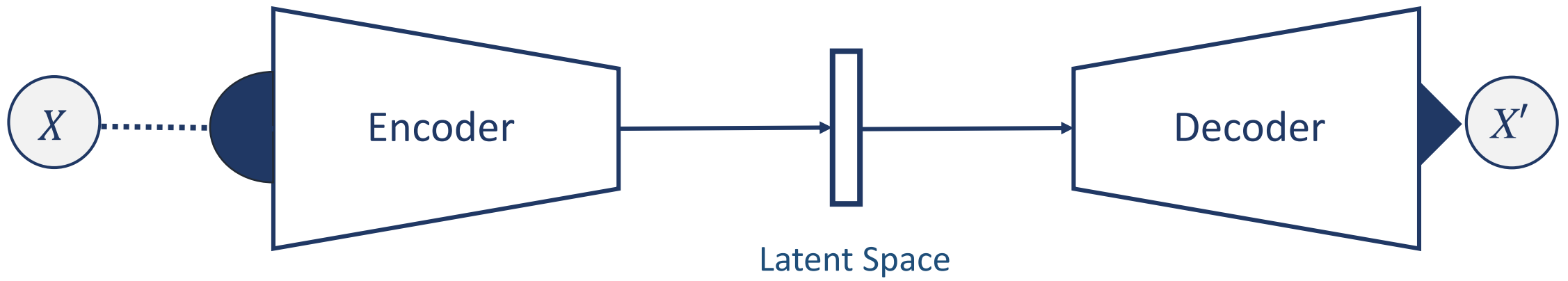
Dimensionality Reduction Method

Generative Model

Probability Model Perspective

# Variational Autoencoders - Background

## Autoencoder Architecture

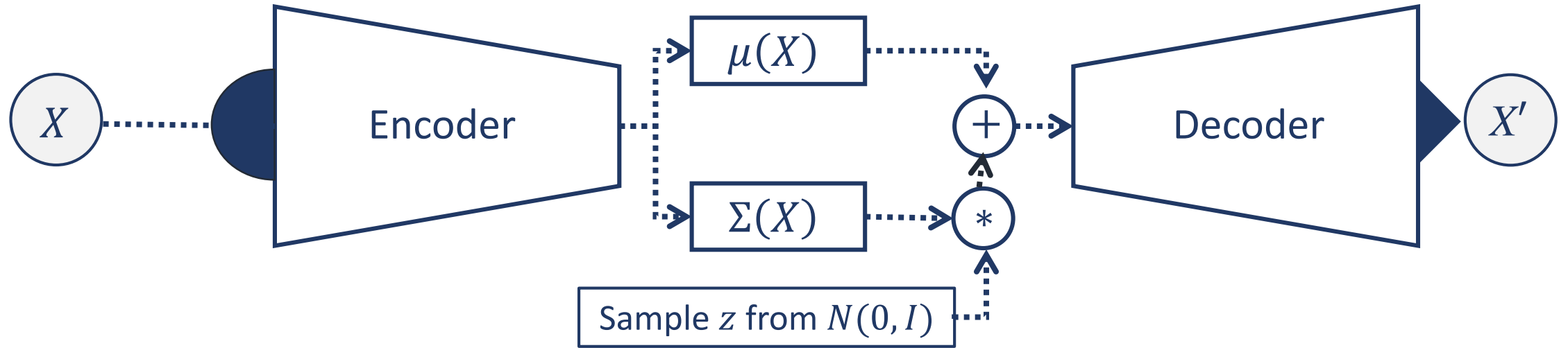


Loss Function

$$\|X - X'\|$$

# Variational Autoencoders - Background

## Variational Autoencoder – Autoencoder with a “twist”

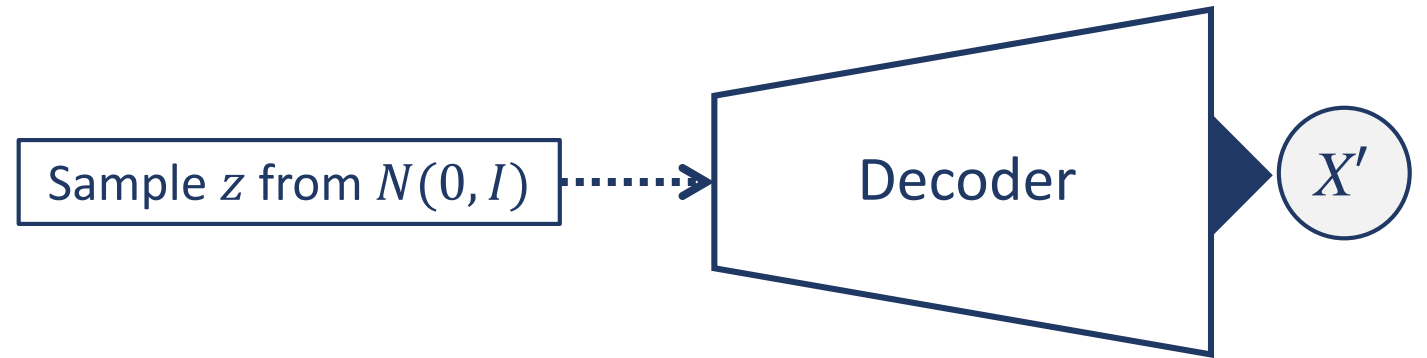


Loss Function

$$\|X - X'\| + \lambda \cdot KL[N(\mu(X), \Sigma(X)) \| N(0, I)]$$

# Variational Autoencoders - Background

## Generative Model



Loss Function

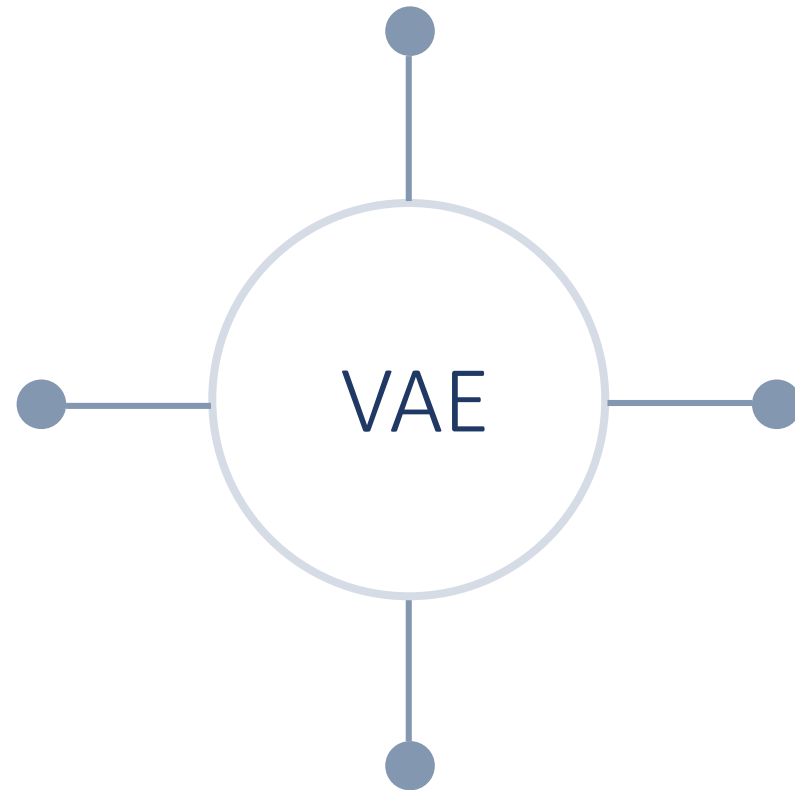
$$\|X - X'\| + \lambda \cdot KL[N(\mu(X), \Sigma(X)) \| N(0, I)]$$



# Variational Autoencoders - Background

Neural Network Perspective

Dimensionality Reduction  
Method



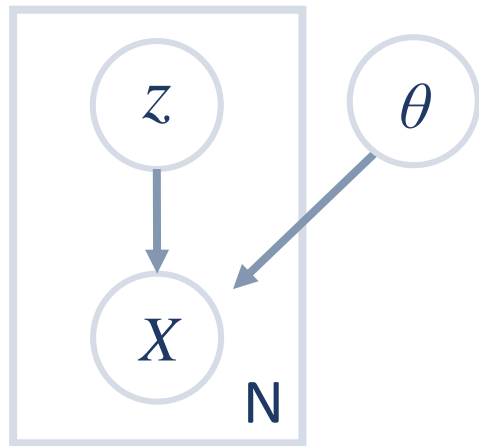
Generative Model

Probability Model Perspective

# Variational Autoencoders - Background

$X$ : training dataset

$z$ : latent variable (w. known prob. distribution,  $z \sim N(0, I)$ )



$$P(X) = \int P(X|z; \theta)P(z)dz \quad (1)$$

Two problems:

1. How to define the latent variables (what information from  $X$  they represent)?
2. How to solve (1)?  $\rightarrow$  Sampling over every possible  $z$ 's is not practical!

# Variational Autoencoders - Background

## 1. How to define the latent variables (what information from $X$ they represent)?

- Assuming a powerful (high-capacity) mapping function  $\theta$ ,  $z$  can be drawn from a simple distribution ( $N(0, I)$ )  $\rightarrow P(z) = N(z|0, I)$
- $f(z; \theta)$  is a deep multi-layer neural network which will map  $z$  to the corresponding  $X$ .

## 2. How solve $P(X)$

- $P(X) = E_{z \sim P(z)} P(X|z)$       Difficult in practice to infer  $P(X|z)$  without sampling a large number of  $z$  values.

To learn a new function  $Q$ , that takes  $X$  and gives a distribution over  $z$  that are likely to produce  $X$ .

- $E_{z \sim Q(z)} P(X|z)$       More practical

$$\begin{array}{c} \downarrow \\ E_{z \sim Q(z)} [\log P(X|z)] \end{array} \stackrel{\text{Bayes' rule}}{=} E_{z \sim Q(z)} [\log P(z|X) + \underbrace{\log P(X)}_{\text{.....}} - \log P(z)]$$

## 2. How solve $P(X)$

$$E_{z \sim Q(z)}[\log P(X|z)] = E_{z \sim Q(z)}[\log P(z|X) + \log P(X) - \log P(z)]$$

Rearranging and subtracting  $E_{z \sim Q(z)}[\log Q(z|X)]$  on both sides...

$$\log P(X) - E_{z \sim Q(z)}[\log Q(z|X) - \log P(z|X)] =$$

$$E_{z \sim Q(z)}[\log P(X|z)] - E_{z \sim Q(z)}[\log Q(z|X) - \log P(z)]$$

Definition of KL divergence  $E_{z \sim Q}[\log a - \log b] = KL[a||b]$

$$\log P(X) - KL[Q(z|X)||P(z|X)] = E_{z \sim Q(z)}[\log P(X|z)] - KL[Q(z|X)||P(z)]$$

# Variational Autoencoders - Background

## 2. How solve $P(X)$

Reconstruction error (Decoder)

$$\log P(X) - \underbrace{KL[Q(z|X)||P(z|X)]}_{\text{Lower bound (KL > 0)}} = \underbrace{E_{z \sim Q(z)}[\log P(X|z)]}_{\text{Reconstruction error (Decoder)}} - \underbrace{KL[Q(z|X)||P(z)]}_{\downarrow}$$

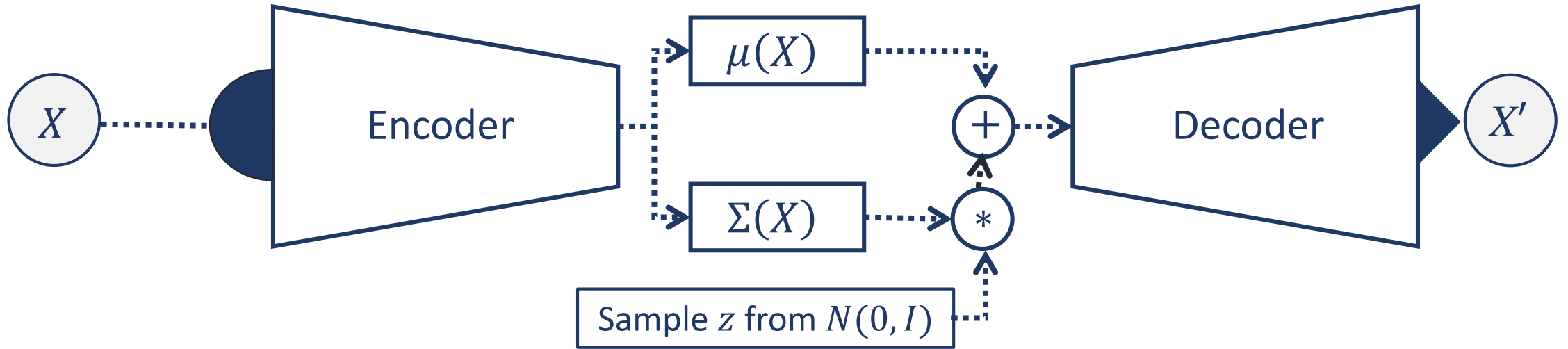
$Q(z|X)$  Gaussian  $\mathcal{N}(\mu, \Sigma)$

KL-div. of two Gaussians  $\rightarrow$  closed form



# Variational Autoencoders - Background

## Reparameterization trick

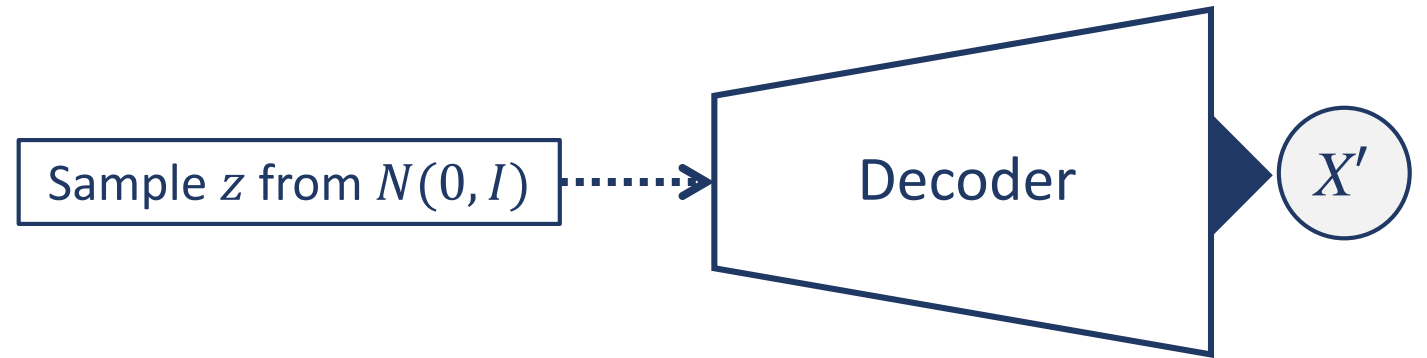


Loss Function

$$\|X - X'\| + \lambda \cdot KL[N(\mu(X), \Sigma(X)) \| N(0, I)]$$

# Variational Autoencoders - Background

## Generative Model



Loss Function

$$\|X - X'\| + \lambda \cdot KL[N(\mu(X), \Sigma(X)) \| N(0, I)]$$



# Conditional Variational Autoencoders - Background

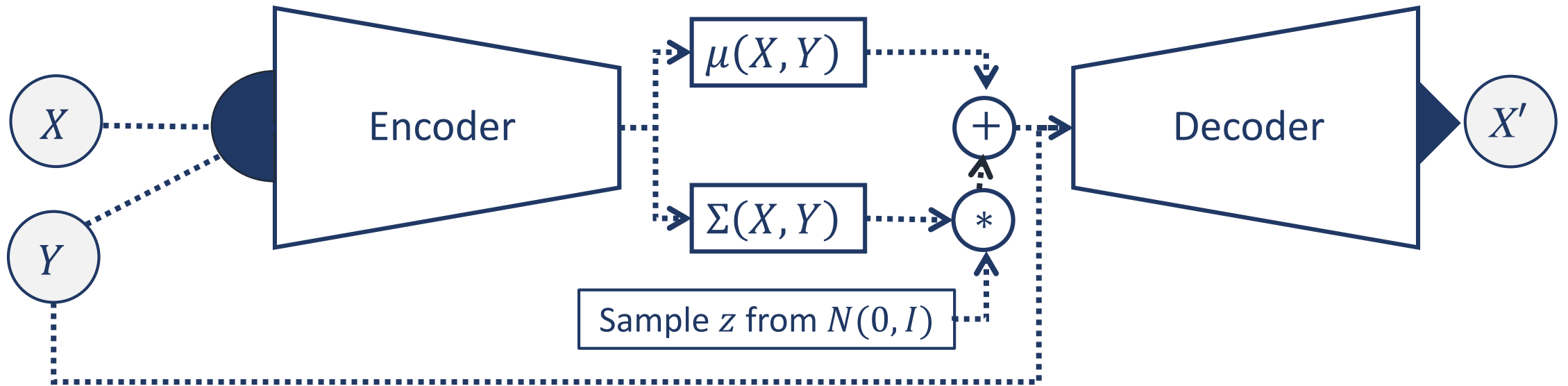
$$P(X) \rightarrow P(X|Y)$$



$$\begin{aligned} \log P(X|Y) - \underbrace{KL[Q(z|X, Y) || P(z|X, Y)]}_{\text{Lower bound (KL > 0)}} &= \underbrace{Q(z|X, Y) \text{ Gaussian } \mathcal{N}(\mu, \Sigma)}_{\text{KL-div. of two Gaussians } \rightarrow \text{closed form}} \\ &= \underbrace{E_{z \sim Q(z)} [\log P(X|Y, z)]}_{\text{Reconstruction error (Decoder)}} - \underbrace{KL[Q(z|X, Y) || P(z|Y)]} \end{aligned}$$

# Conditional Variational Autoencoders - Background

## Reparameterization trick

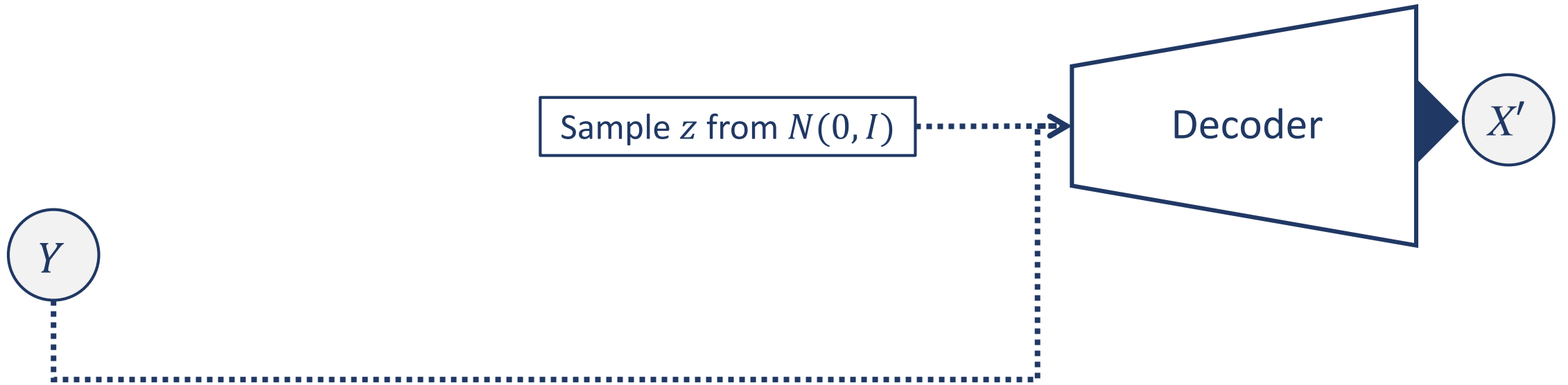


Loss Function

$$\|X - X'\| + \lambda \cdot KL[N(\mu(X, Y), \Sigma(X, Y)) \| N(0, I)]$$

# Conditional Variational Autoencoders - Background

## Reparameterization trick

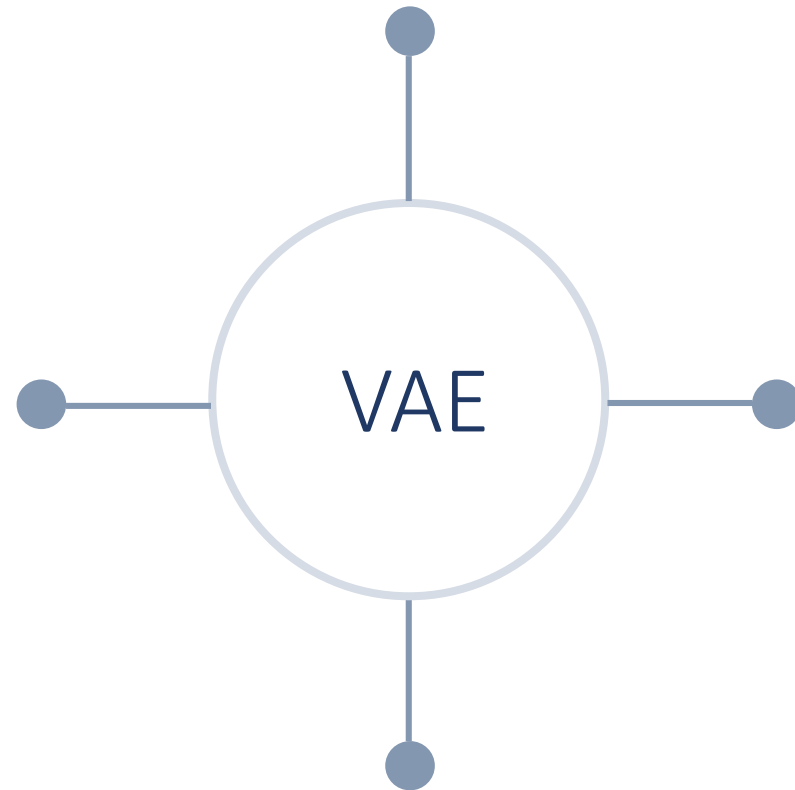


Loss Function

$$\|X - X'\| + \lambda \cdot KL[N(\mu(X, Y), \Sigma(X, Y)) \| N(0, I)]$$

# Variational Autoencoders - Background

Neural Network Perspective

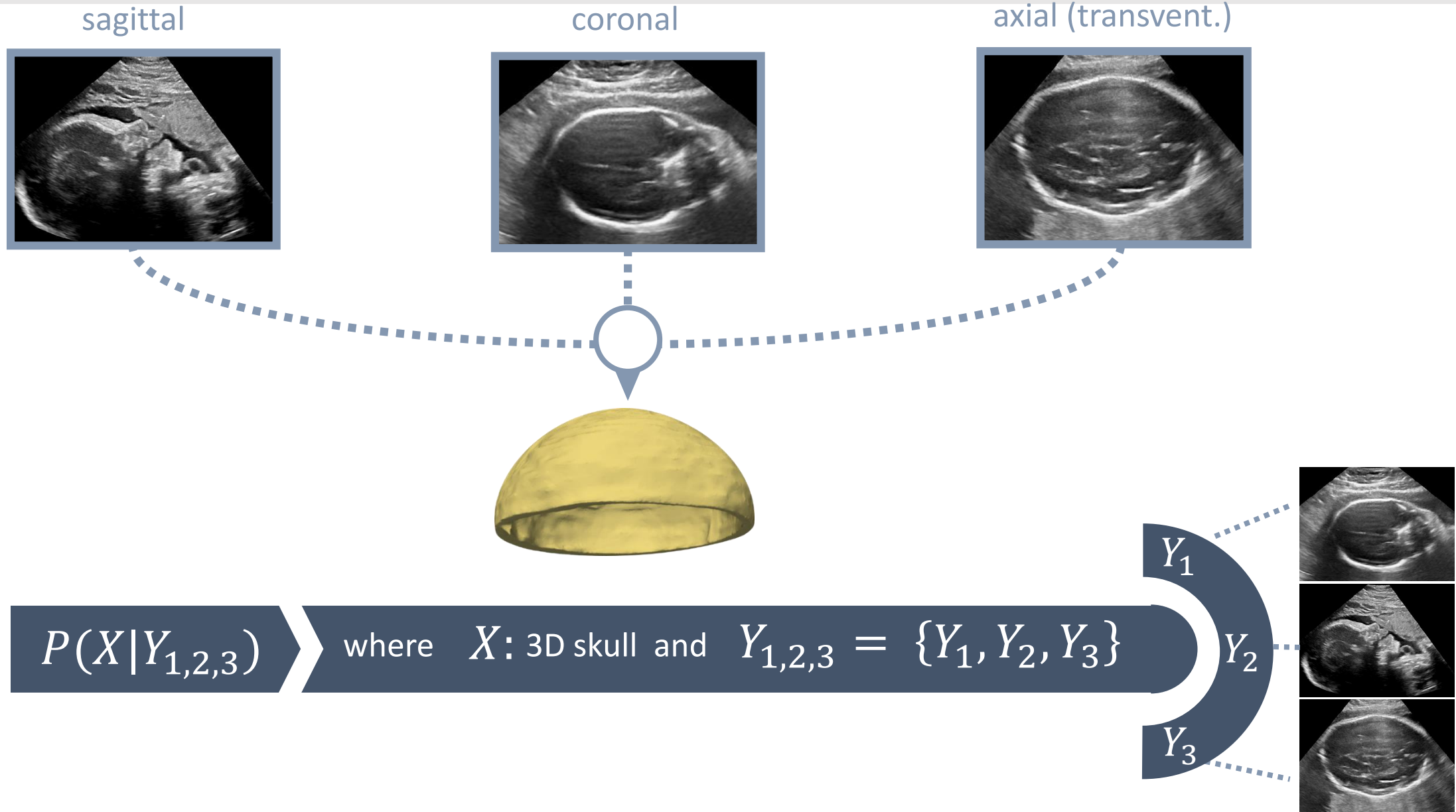


Generative Model

Dimensionality Reduction  
Method

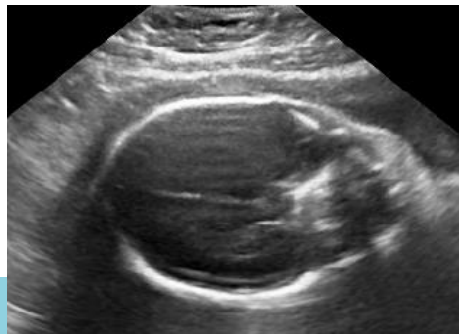
Probability Model Perspective

# 3D Anatomy Reconstruction from 2DUS





Sagittal



Coronal



Transcerebellar



Transventricular

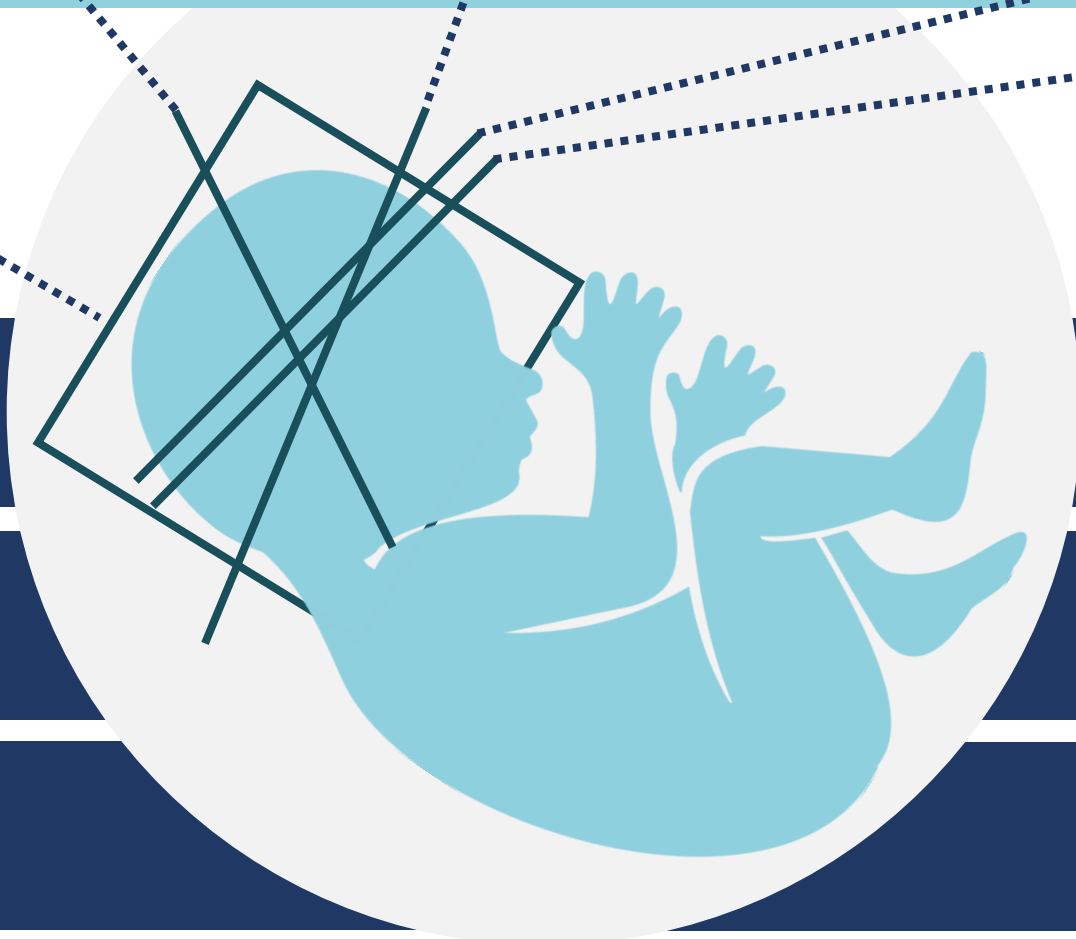


Transthalamic

Standard planes manually acquired.

2D Biometrics.

Manual measurements.



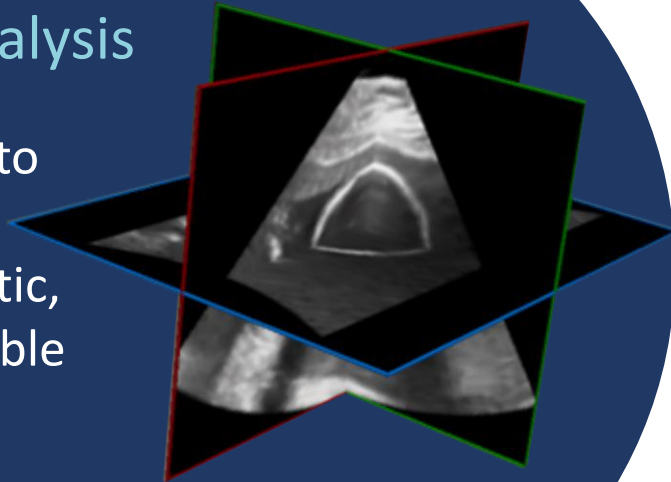
Low reproducibility

Subjectivity

Prone to errors.

## Towards 3D Fetal Analysis

3D US has the potential to mitigate these effects, providing a more realistic, objective, and reproducible analysis tool.



## 3D vs 2D



Dyson et al. "Three-dimensional ultrasound in the evaluation of fetal anomalies" *Ultrasound Obstet. Gynecol.* 2000, 16.



Basgul et al. "Evaluation of fetal anomalies by two and three-dimensional ultrasound" *Gynaecol Perinatol* 2007, 16(2).



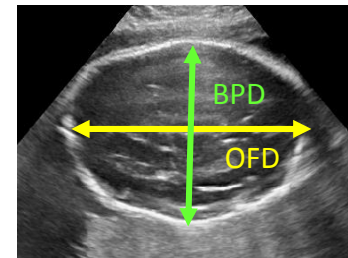
Lee et al. "A review of three-dimensional ultrasound applications in fetal growth restriction" *Journal of Medical Ultrasound* 2012, 20.



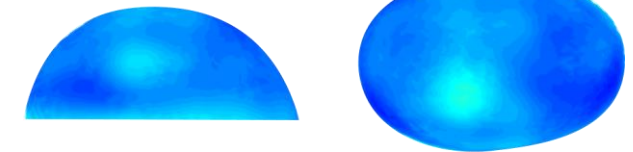
Goncalves et al. "Three- and 4-dimensional ultrasound in obstetric practice: Does it help?" *J Ultrasound Med.* 2005, 24



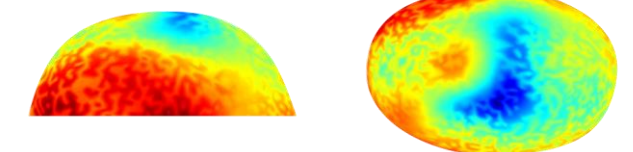
Goncalves et al. "What does 2-dimensional imaging add to 3- and 4-dimensional obstetric ultrasonography?" *J Ultrasound Med* 2006, 25.



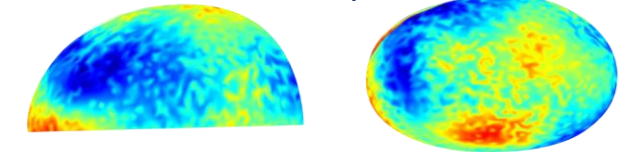
normal



dolichocephalic



dolichocephalic



## 3D Biometry for Fetal Skull Assessment

J. Matthew et al. "Novel 3D-based metric to assess the fetal skull: A Pilot Study. *BMUS* 2017.

# Towards 3D Fetal Analysis

2D

3D

## Analysis and Visualization

### Automatic Tools for Segmentation and Analysis

Cerrolaza et al. "Deep learning with ultrasound physics for fetal skull segmentation" ISBI 2018

Namburete et al. "Fully-automated alignment of 3D fetal brain ultrasound to a canonical reference space using multi-task learning" Med. Image Anal. 2018

## Limited Experience

### Automatic Detection of Anatomical Structures and Standard Planes in 3DUS

Li et al. "Standard plane detection in 3D fetal ultrasound using an iterative transformation network" MICCAI 2018

Huang et al. "VP-Nets: Efficient automatic localization of key brain structures in 3D fetal neurosonography" Med. Image Anal. 2018,47

## Lack of Large Dataset

Need of large international/ multi-ethnic studies to create new reference charts for 3D biometry





Not all the standard views are always routinely acquired

## Hierarchical CVAE



Axial (Transvent.)



Always acquired.  
Classic 2D biometrics.



Sagittal



Frequently.  
Face / head shape.



Coronal

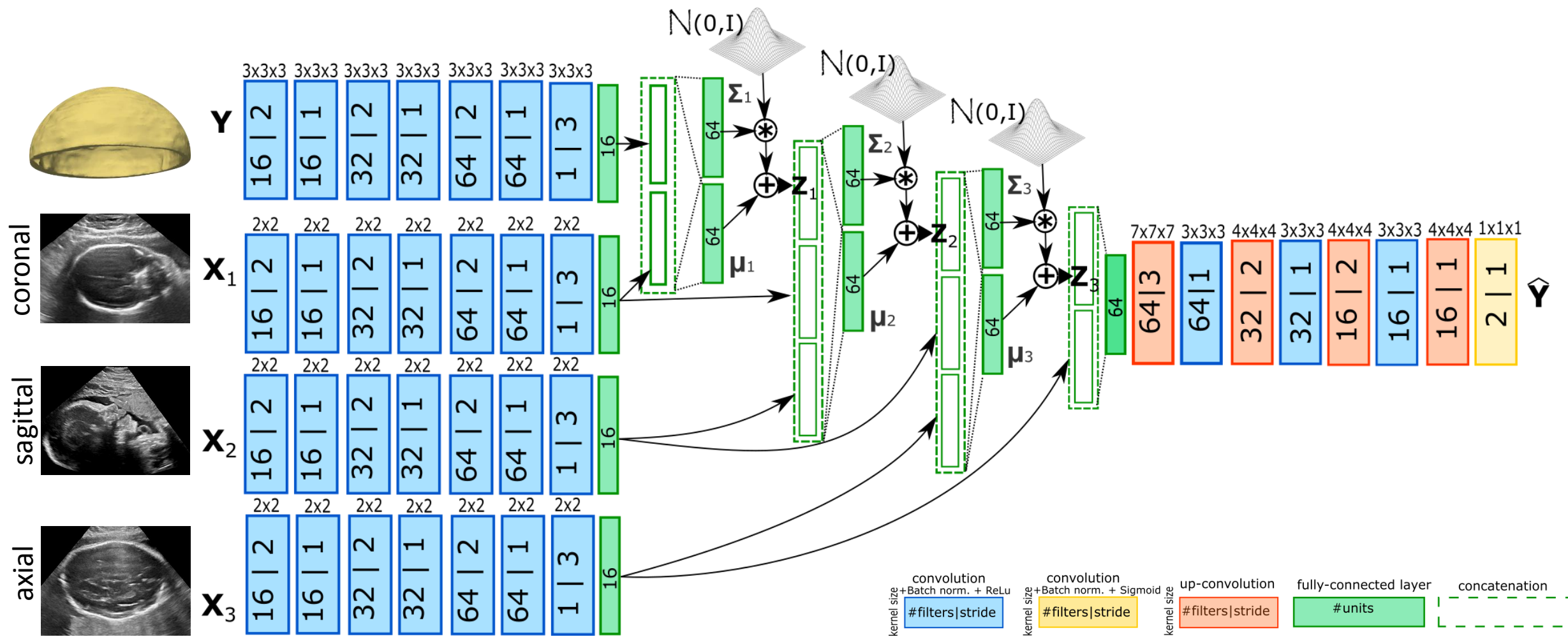


Sometimes.  
Normally acquired as part of a  
dedicated scan.



# 3D Anatomy Reconstruction from 2DUS

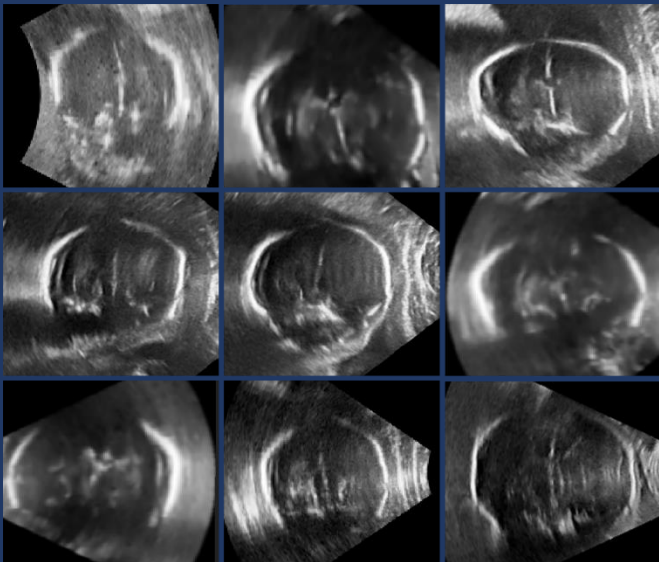
## Conditional Variational Autoencoders for 3D Fetal Anatomy Reconstruction



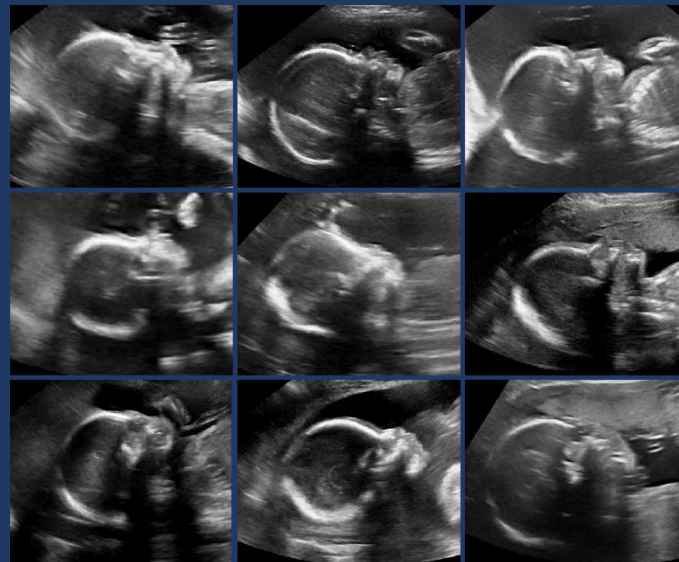
## Experiments

- Data: 72 cases (IBD approved); avg. gest. age 24.7 (20 to 36 weeks)  
58 training / 14 testing (3-folds)
- Preprocessing: Resized to 96 x 96 x 96 vox. (96 x 96 pixels); isotropic 0.50 mm
- 3D skull manually segmentation supervised by expert radiologist.
- Random anisotropic scaling, rotations ( $\pm 10^\circ$ ) and translations ( $\pm 7$  pix.).
- Adam (l.r. = 0.001,  $\beta_1=0.9$ ,  $\beta_2=0.995$ ); 1000 epochs.

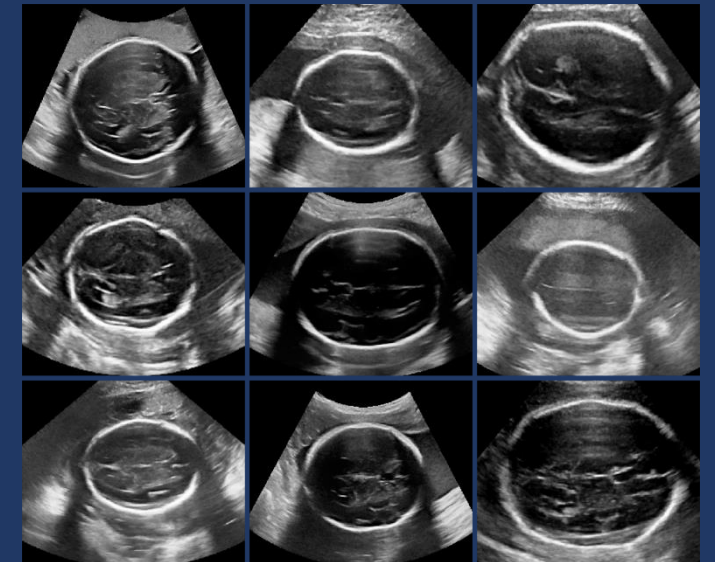
Coronal



Sagittal

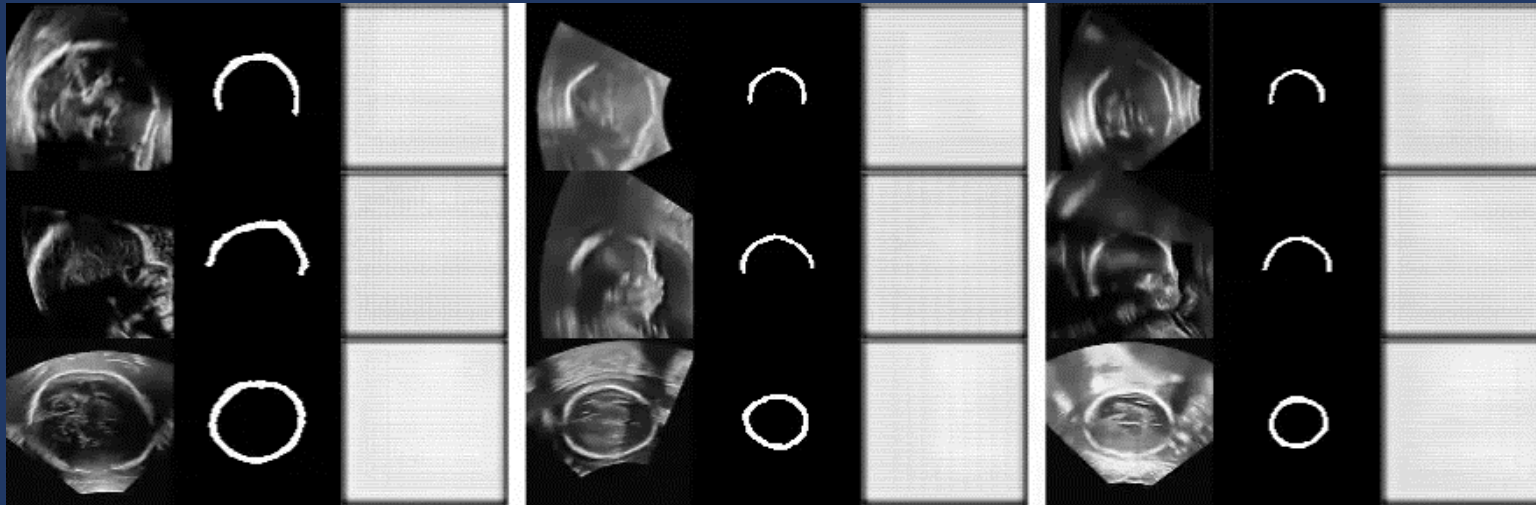


Axial (transvent.)

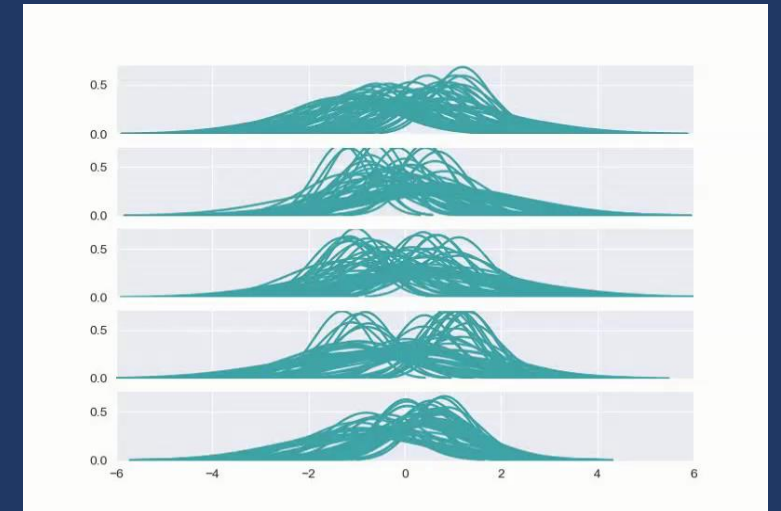


Training progress...

## Skull reconstruction



## Latent space



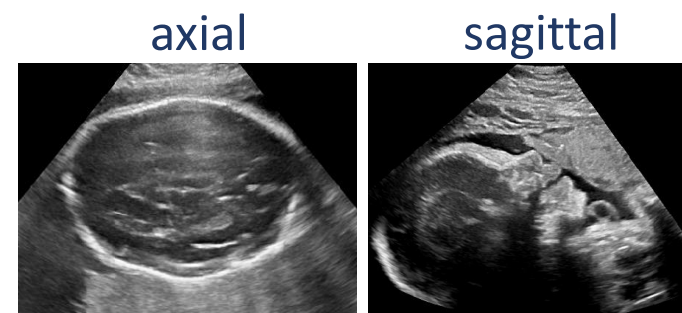


DC: Dice coeff. HD: Hausdorff dist. (mm). RVD: Relative volume diff.

	DC	HD	RVD
CVAE	0.91 ± 0.02	4.33 ± 1.71	0.03 ± 0.12
<b>HCVAE</b>	<b>0.91 ± 0.04</b>	<b>4.12 ± 1.98</b>	<b>0.03 ± 0.14</b>
TL-NET [4]	0.89 ± 0.03	4.79 ± 1.28	0.09 ± 0.17
GAN	0.89 ± 0.04	5.16 ± 1.5	0.03 ± 0.16



	DC	HD	RVD
CVAE	0.86 ± 0.05	5.43 ± 2.78	0.03 ± 0.30
<b>HCVAE</b>	<b>0.89 ± 0.05</b>	<b>4.81 ± 2.44</b>	<b>0.03 ± 0.20</b>
TL-NET [4]	0.89 ± 0.05	5.32 ± 1.99	0.09 ± 0.19
GAN	0.86 ± 0.07	5.93 ± 2.66	0.05 ± 0.30



	DC	HD	RVD
CVAE	0.83 ± 0.06	6.23 ± 2.88	0.09 ± 0.33
<b>HCVAE</b>	<b>0.86 ± 0.05</b>	<b>5.04 ± 2.82</b>	<b>0.04 ± 0.21</b>
TL-NET [4]	0.85 ± 0.04	7.04 ± 2.34	0.17 ± 0.20
GAN	0.83 ± 0.08	8.04 ± 3.06	0.17 ± 0.37

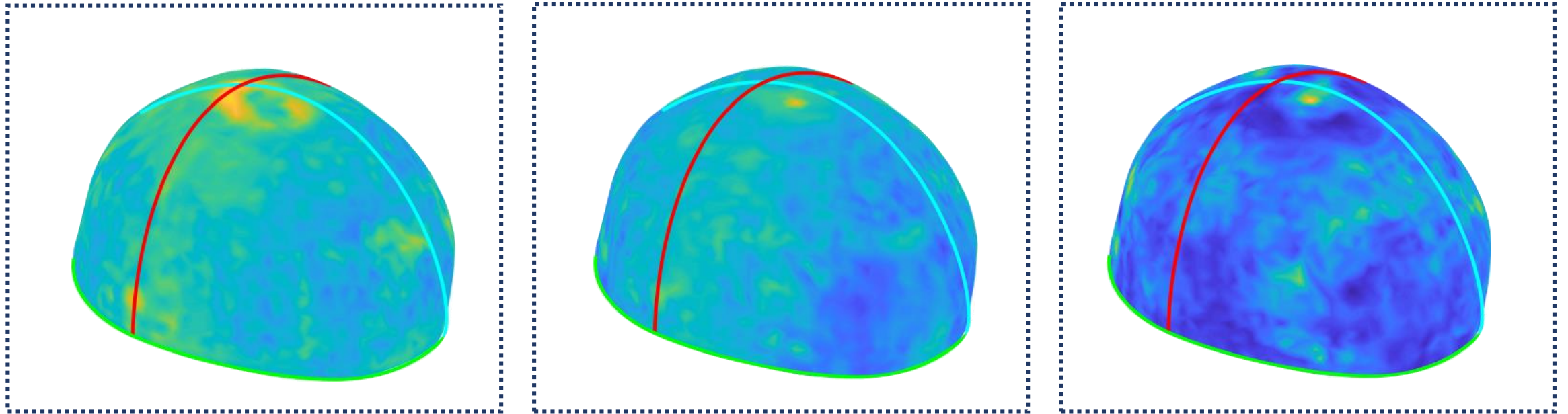


# Prediction Uncertainty in HCVAE

axial

axial + sagittal

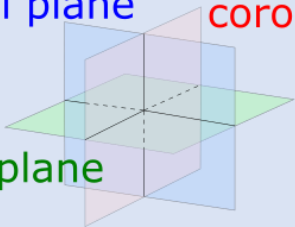
axial + sagittal + coronal



sagittal plane

coronal plane

axial plane



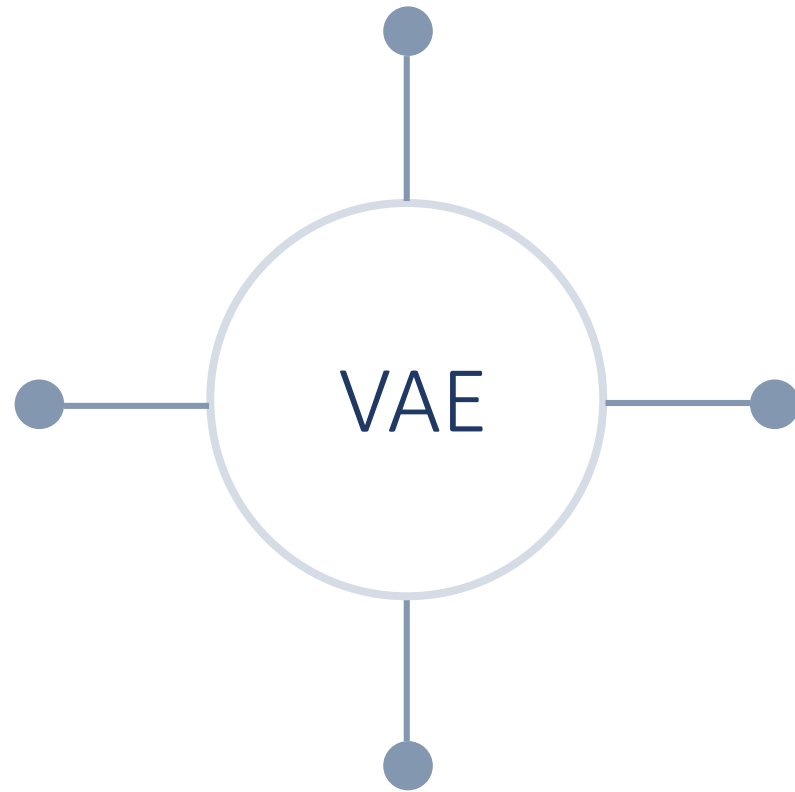
prediction standard deviation (mm)

0.2 0.4 0.6 0.8 1.0 1.2 1.4 1.6

# Variational Autoencoders - Background

Neural Network Perspective

Dimensionality Reduction  
Method



Generative Model

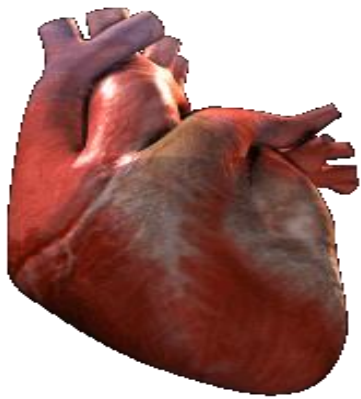
Probability Model Perspective

# Explainable Cardiac Remodeling Assessment

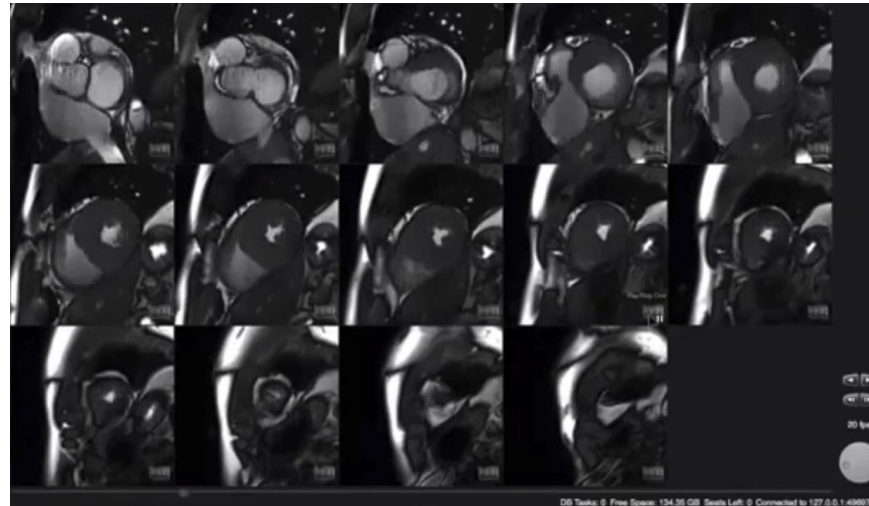
## Cardiac remodeling

- refers to any change in size and shape of the heart
- strong predictor of survival in cardiac pathologies.

Cardiovascular magnetic resonance (CMR) has become the gold-standard for high-resolution imaging of the cardiac structure.



Biological Ground Truth



Left Ventricular (LV) short-axis cine MR acquisition

SAX3D Stack LV Function	
EDV:	119 ml
ESV:	42 ml
SV:	78 ml
EF:	65 %
CO:	4805 ml/min
CI:	2 l/min/m <sup>2</sup>
HR:	62.0/min
Myo Mass (Diast):	96 g
Phase Diastole:	1
Phase Systole:	12
EDV/H:	64 ml/m
EDV/BSA:	59 ml/m <sup>2</sup>
ESV/H:	22 ml/m
ESV/BSA:	21 ml/m <sup>2</sup>
SV/H:	42 ml/m
SV/BSA:	38 ml/m <sup>2</sup>
Myo Mass/H (Diast):	52 g/m
Myo Mass/BSA (Diast):	48 g/m <sup>2</sup>

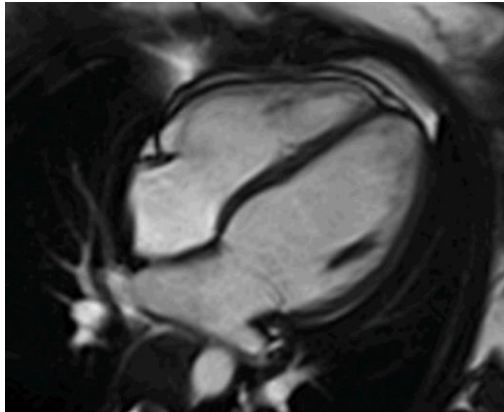
Clinical Indexes



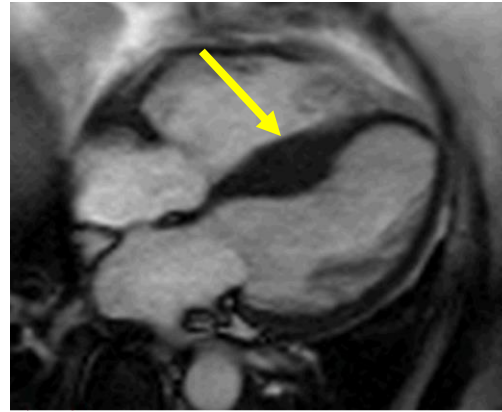
# Explainable Cardiac Remodeling Assessment

## Hypertrophic Cardiomyopathy (HCM)

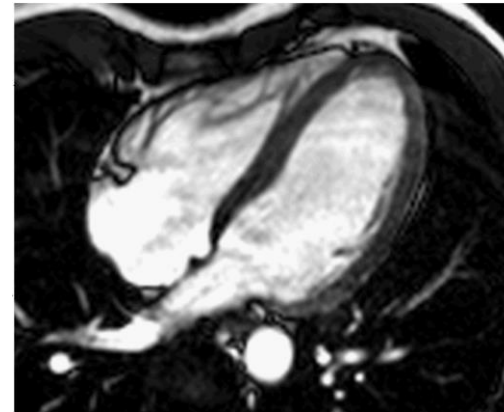
Disease of the heart muscle which manifests clinically with unexplained left ventricular (LV) **hypertrophy** (thickening).



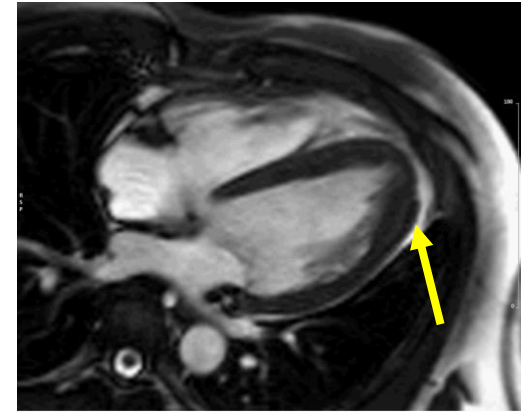
Healthy



HCM



Healthy



HCM

Conventional clinical indexes are insensitive to **regional** and **asymmetrical** remodeling.

# Explainable Cardiac Remodeling Assessment

## Hypertrophic Cardiomyopathy (HCM) – Shape Descriptors

### PCA shape components

- 😊 Easy to **visualize**.
- 😞 Just summarizes data variability → they **do not** necessarily encode anatomical features that can **differentiate** between classes.

### Machine Learning approaches

- 😊 Powerful feature extraction.
  - 😞 Lack interpretability
- ➔ VAE

Learns a set of latent variables  $z$  that:

1. can **differentiate** clinical conditions  $y$ .
2. and whose anatomical effect can be **visualized**.

# Explainable Cardiac Remodeling Assessment

## Hypertrophic Cardiomyopathy (HCM) – Shape Descriptors

- End-diastolic (ED) and end-systolic (ES) phases of cardiac cine MR images of healthy (HVols) and HCM subjects were automatically segmented<sup>1</sup>.
- 3D segmentations quality was improved by a multi-atlas-aided upsampling scheme and ED and ES frames were registered to a common template.

### IMPERIAL COLLEGE DATASET:

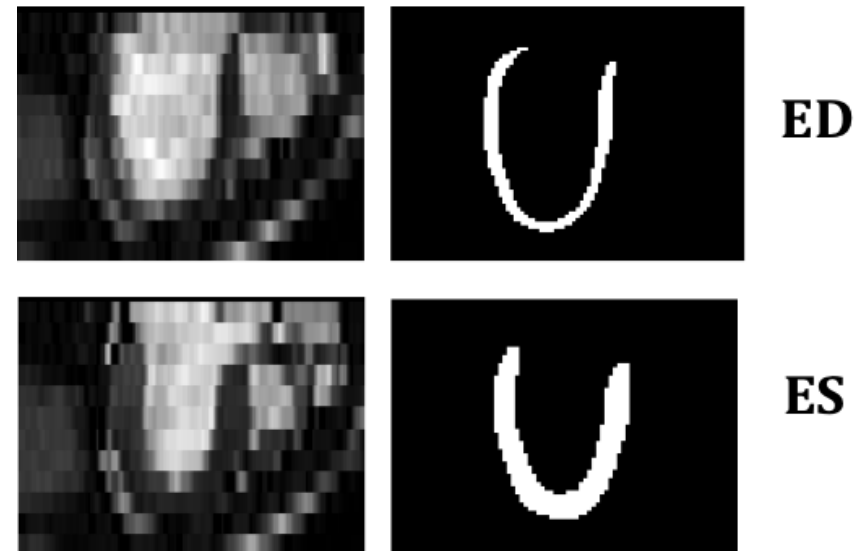
**TRAINING:** 537 (276 HVols, 261 HCMs)

**VALIDATION:** 150 (75 HVols, 75 HCMs)

**TESTING:** 200 (200 HVols, 200 HCMs)

### ACDC MICCAI 2017 DATASET:

**TESTING:** 40 (20 HVols, 20 HCMs)



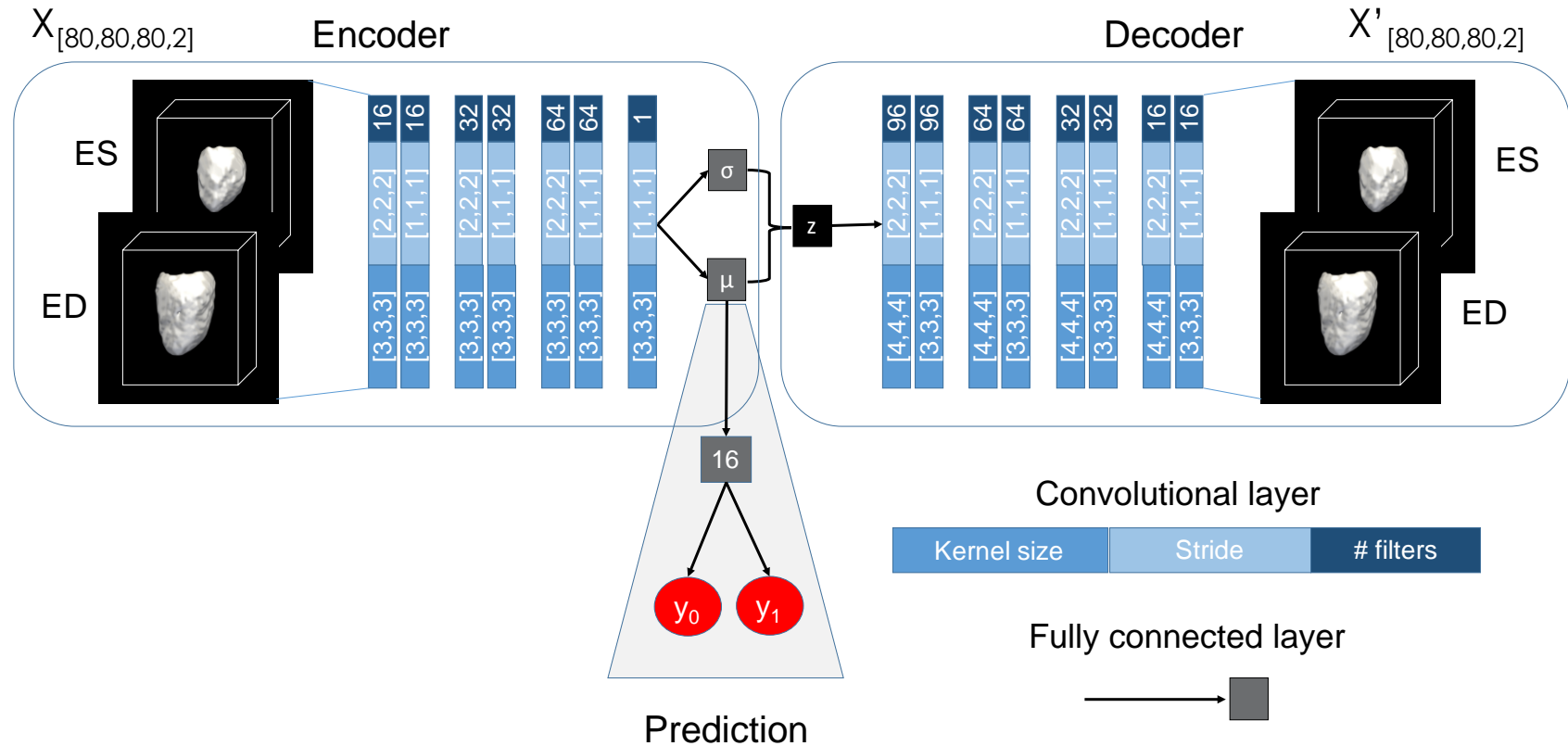
Exemplar 2D LV short-axis views and corresponding LV segmentation at ED and ES.

<sup>1</sup>Bai, W. et al. *A bi-ventricular cardiac atlas built from 1000+ high resolution MR images of healthy subjects*. *MedIA* 2015 Dec;26(1):133-45.

# Explainable Cardiac Remodeling Assessment

## Hypertrophic Cardiomyopathy (HCM) – Shape Descriptors

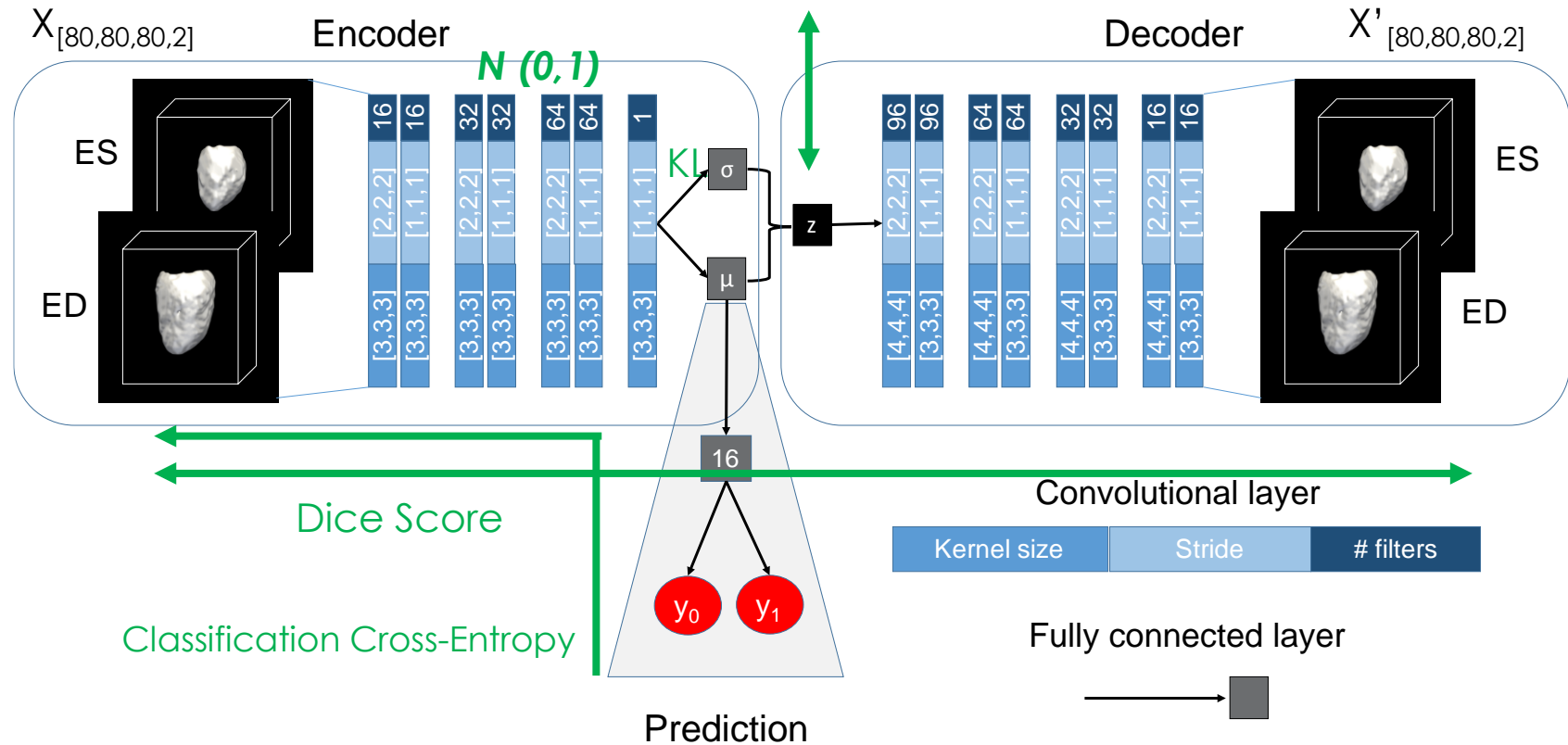
### VAE Implementation



# Explainable Cardiac Remodeling Assessment

## Hypertrophic Cardiomyopathy (HCM) – Shape Descriptors

### VAE Implementation

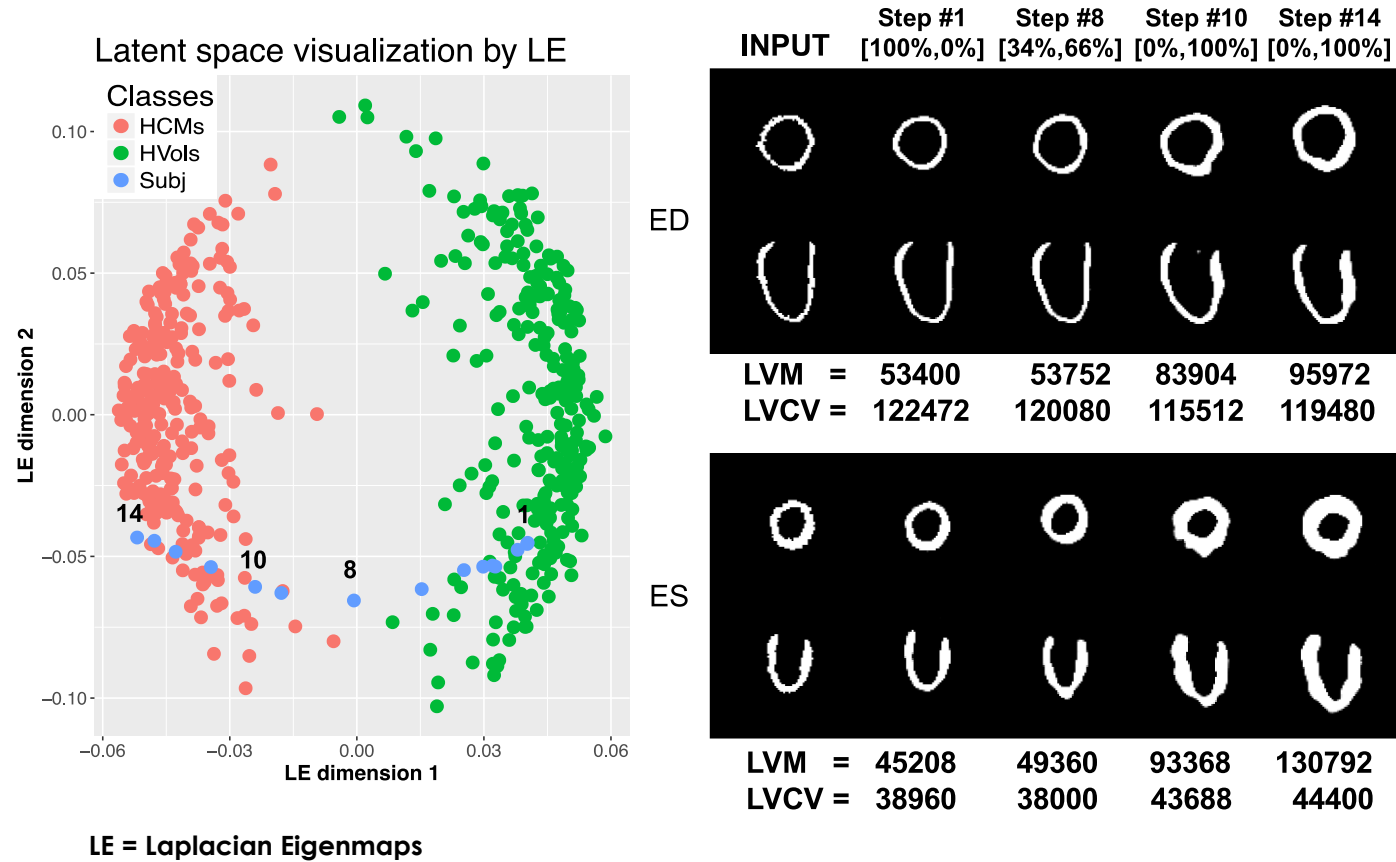


**Latent Space Navigation:** 
$$\mu_t = \mu_{t-1} + \lambda \frac{\delta y_1}{\delta \mu_{t-1}}$$
  $t = \text{iteration number}, \lambda=0.1$

# Explainable Cardiac Remodeling Assessment

## Hypertrophic Cardiomyopathy (HCM) – Shape Descriptors

### VAE Implementation



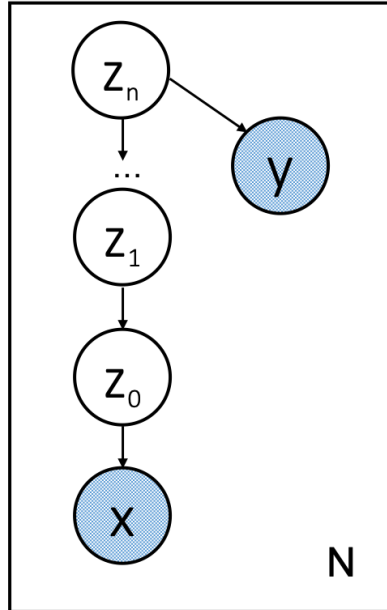
TESTING – IMPERIAL COLLEGE DATASET: 200 (100 HVols, 100 HCMs) – 100% accuracy  
– ACDC MICCAI 2017: 40 (20 HVols, 20 HCMs) – 90% accuracy

# Explainable Cardiac Remodeling Assessment

## Hypertrophic Cardiomyopathy (HCM) – Shape Descriptors

### Can we do even better?

- Latent space navigation is subject-specific, i.e. no population-based inference.
- Latent space can only be visualized with an additional dimensionality reduction technique.



Given a population of  $N$  shapes  $X$ , we aim at developing a data-driven method that learns a conditional hierarchy of latent variables  $\{z_N, \dots, z_1, z_0\}$  where:

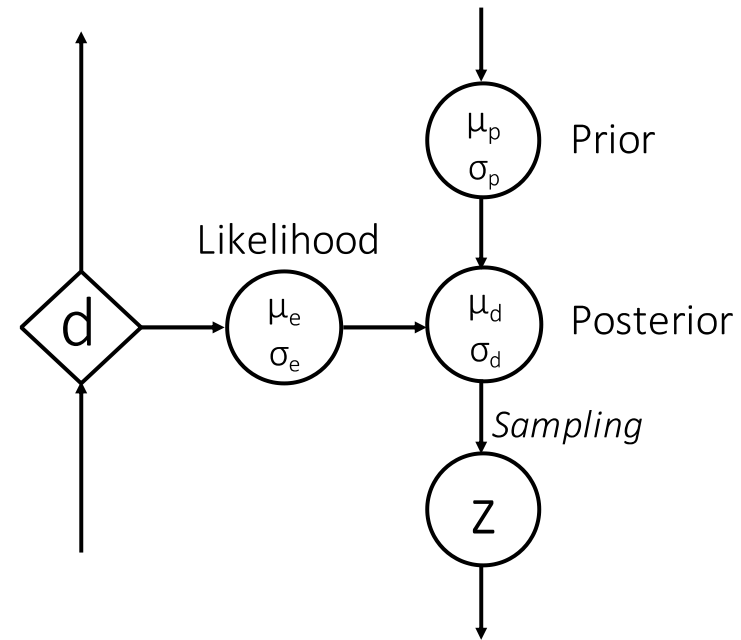
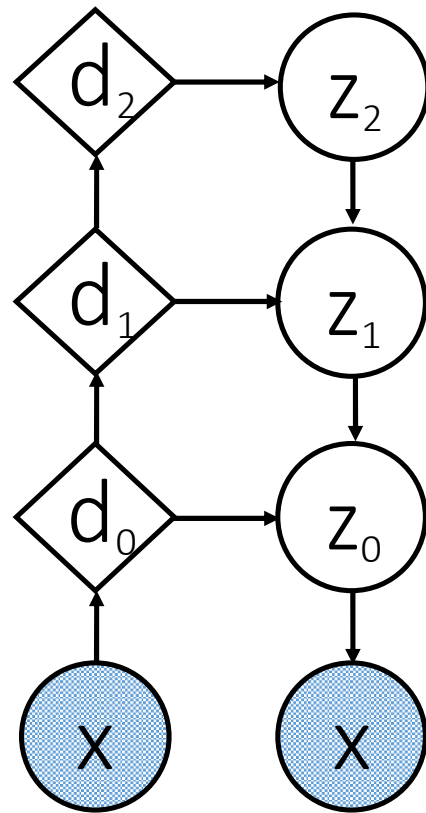
1.  $z_N$  can **differentiate between** clinical conditions  $y$  and is very **low-dimensional**.
2.  $\{z_N, \dots, z_1, z_0\}$  anatomical effect can be **visualized**.

# Explainable Cardiac Remodeling Assessment

## Hypertrophic Cardiomyopathy (HCM) – Shape Descriptors

### Ladder VAE

*Novelty:* Sharing of information between encoder and decoder.



$$\mu_d = \frac{\mu_e \sigma_e^{-2} + \mu \sigma_p^{-2}}{\sigma_e^{-2} + \sigma_p^{-2}}$$

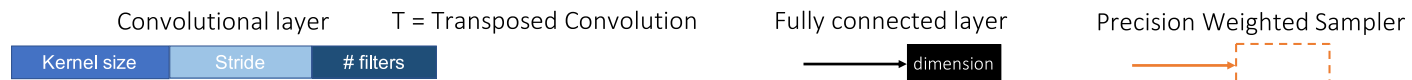
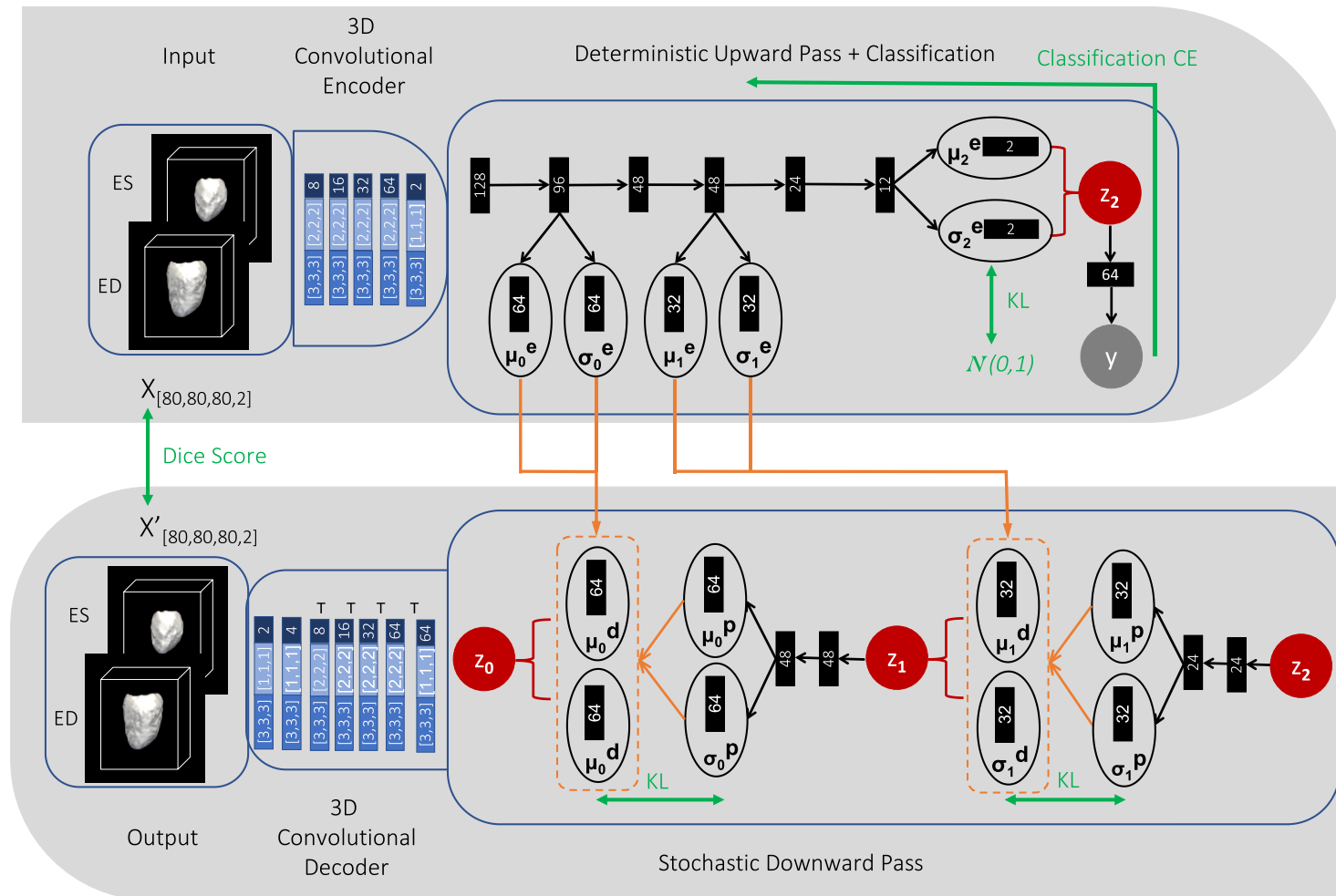
$$\sigma_d^2 = \frac{1}{\sigma_e^{-2} + \sigma_p^{-2}}$$



# Explainable Cardiac Remodeling Assessment

## Hypertrophic Cardiomyopathy (HCM) – Shape Descriptors

### Ladder VAE



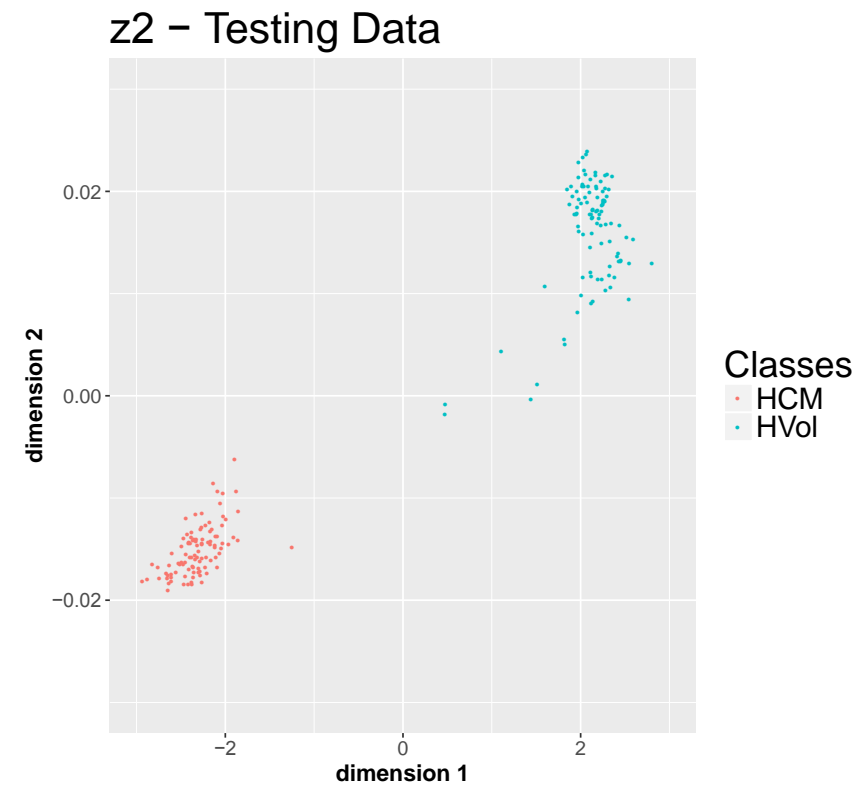
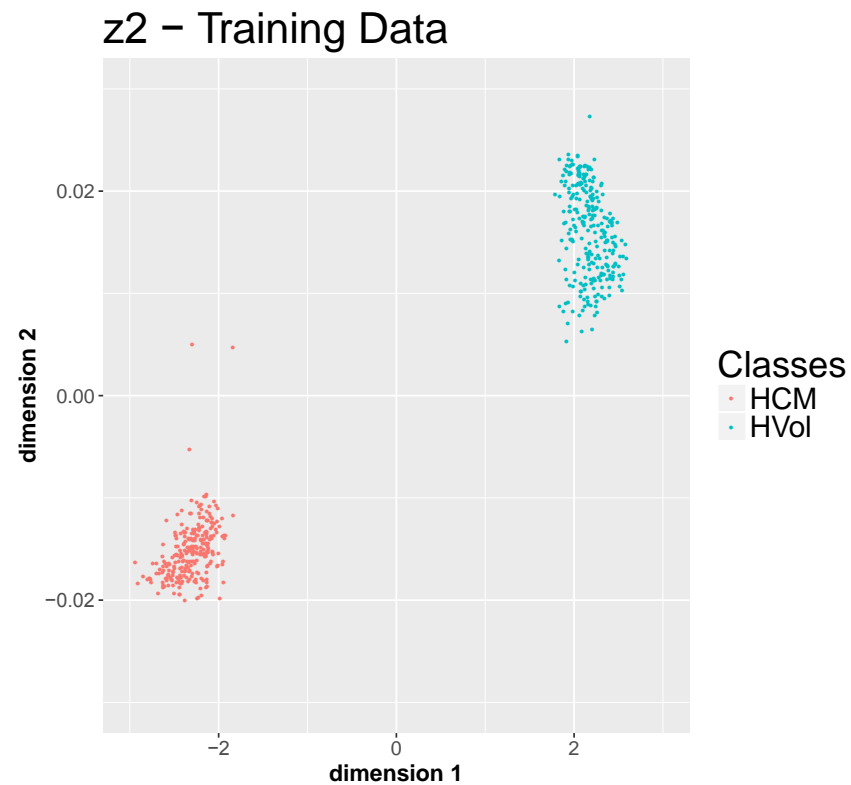
# Explainable Cardiac Remodeling Assessment

## Hypertrophic Cardiomyopathy (HCM) – Shape Descriptors

### Ladder VAE

TESTING – IMPERIAL COLLEGE DATASET: 200 (100 HVols, 100 HCMs) – 100% accuracy

– ACDC MICCAI 2017: 40 (20 HVols, 20 HCMs) – 90% accuracy

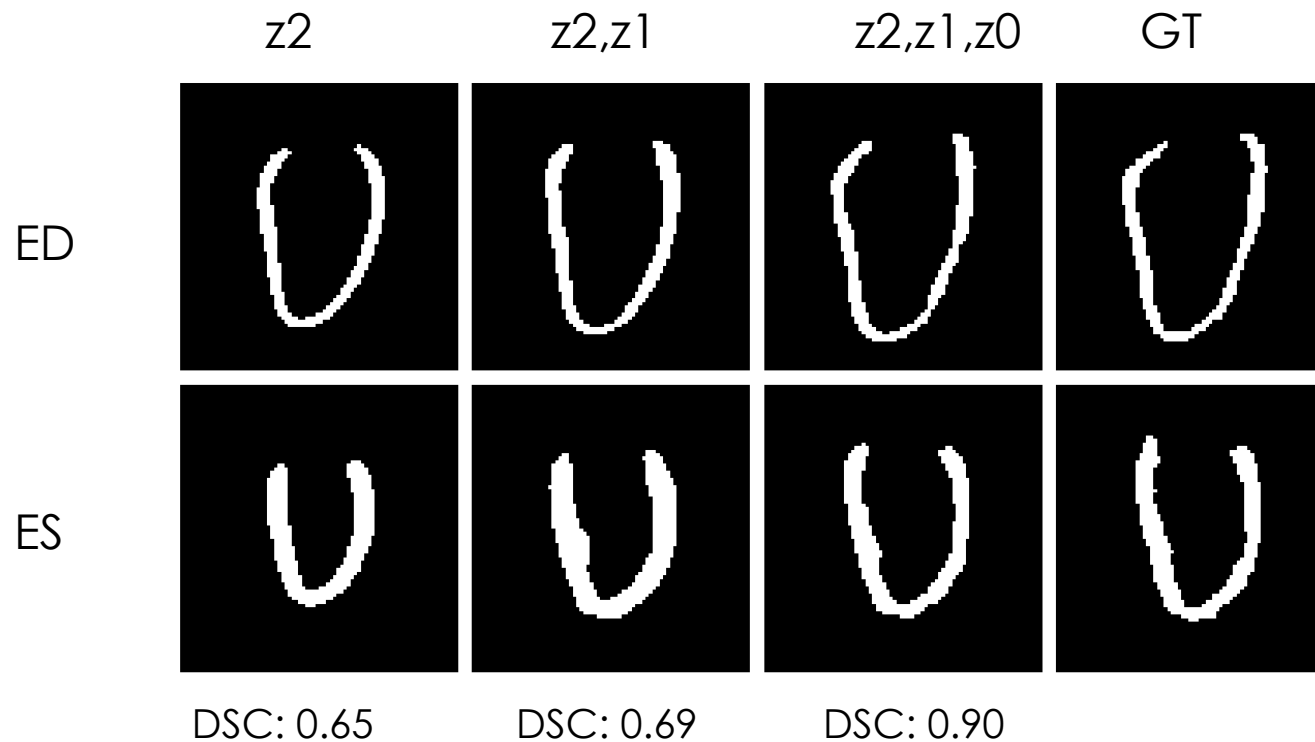


# Explainable Cardiac Remodeling Assessment

## Hypertrophic Cardiomyopathy (HCM) – Shape Descriptors

### Ladder VAE

VAE vs LVAE Reconstruction Accuracy				
	$DSC_{ED}$	$DSC_{ES}$	$H_{ED}[mm]$	$H_{ES}[mm]$
VAE	$0.71 \pm 0.07$	$0.78 \pm 0.06$	$4.87 \pm 1.23$	$5.09 \pm 1.51$
LVAE	$0.79 \pm 0.06$	$0.84 \pm 0.05$	$3.92 \pm 1.08$	$4.09 \pm 1.36$

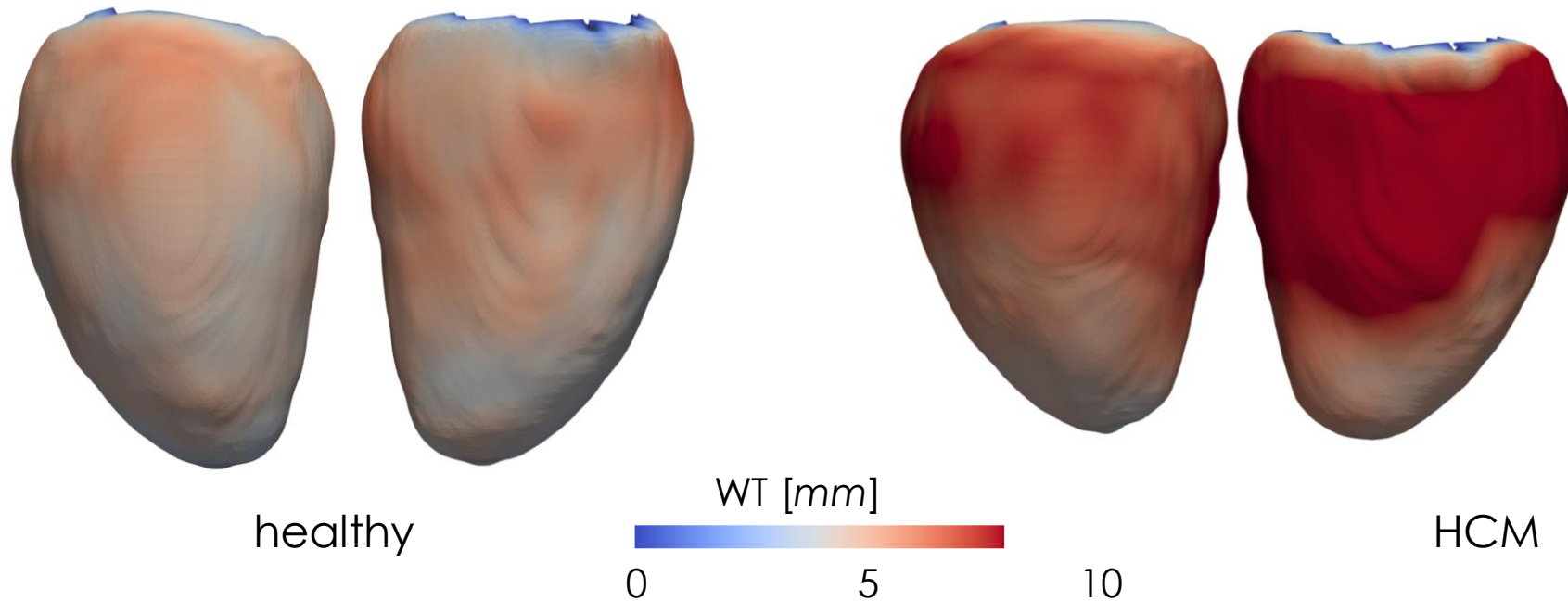


# Explainable Cardiac Remodeling Assessment

## Hypertrophic Cardiomyopathy (HCM) – Shape Descriptors

### Ladder VAE

Mean healthy and HCM shapes generated by sampling from  $z_2$  clusters.  
Wall Thickness (WT) values are plotted at each vertex.



HCM shapes has ~15% greater mass and ~6% bigger cavity volume.

# Conclusions

- VAEs are **NOT just a particular subgroup of autoencoders** with a Bayesian “twist”.
- VAEs is a versatile, and flexible family of networks with a solid **foundation in probability theory**.
- Their **intrinsic duality** as **dimensionality reduction** network and **generative models** make them an interesting approach for solving different problems in medical imaging.
- Potential of deep generative networks for the **3D reconstruction of the fetal skull** from non-registered 2DUS standard planes → **New generation of 3D fetal biometry**
- New approach as visualization and classification technique for cardiac pathologies.

# Artificial Intelligence for Science, Industry, and Society

## AISIS - 2019

Thank You!

Juan J. Cerrolaza, PhD  
accenturetechnology  
artificialintelligence IBERIA



Imperial College  
London



Children's National™

Sheikh Zayed Institute  
for Pediatric Surgical Innovation  
Part of the Children's National Health System

accenture